EFFECT OF FIBRE ORIENTATION ON THE TENSILE STRENGTH OF ULTRA-HIGH PERFORMANCE STEEL FIBRE-REINFORCED SELF-COMPACTING CONCRETE

Wilson R. Leal da Silva (1), Oldrich Svec (1), Lars N. Thrane (1), Claus Pade (1)

(1) Danish Technological Institute, Gregersensvej 4, 2630 Taastrup, DK

Abstract

Fibre orientation has a significant impact on the mechanical properties of fibre reinforced concrete. Experimental studies indicate that there exists a prevailing linear relation between the fibre orientation factor and the corresponding tensile strength of the material. This paper extends the knowledge of fibre orientation and its influence on tensile strength to the field of ultra-high performance steel fibre-reinforced self-compacting concrete (UHPSFRSCC). For that, a slab produced with UHPSFRSCC was cast and cut into cubic samples (cross section: 75 × 75 mm). Ten selected samples were tested by means of a custom designed direct-tensile strength test method. Subsequently, an image analysis algorithm identified the number of fibres on the samples' fracture plane, allowing for computing the corresponding local fibre orientation factor. Finally, the fibre orientation factor was correlated to tensile strength test results, composing a set of design charts fit for design applications.

Résumé

L'orientation des fibres a une influence importante sur les propriétés mécaniques des bétons de fibres. Les études expérimentales montrent qu'il existe une loi linéaire qui régit la relation entre le facteur d'orientation des fibres et la résistance en traction correspondante du matériau. L'article étend cette connaissance de l'influence de l'orientation des fibres sur la résistance en traction au domaine des bétons de fibres d'acier à ultra-hautes performances autoplaçants. A cet effet, une dalle constituée d'un tel BFUP autoplaçant a été coulée et découpée en éprouvettes cubiques de section 75 × 75 mm. Dix échantillons ont été sélectionnés pour être testés selon une méthode spécialement mise au point pour déterminer leur résistance en traction directe. Ensuite, le nombre de fibres traversant le plan de rupture des échantillons a été identifié grâce à un algorithme d'analyse d'images, ce qui a permis de calculer le facteur d'orientation des fibres local correspondant. Enfin, le facteur d'orientation des fibres a été relié au résultat expérimental de résistance en traction, constituant un jeu d'abaques adapté à une utilisation par le concepteur.

1. INTRODUCTION

The composition of Ultra-High Performance Steel Fibre-Reinforced Self-Compacting Concrete (UHPSFRSCC) and interaction between the fibres and the matrix in post-peak state, i.e. after cracking, adds complexity to the prediction of the mechanical behaviour of structural elements produced with such concrete type. As an example, UHPSFRSCC cannot be assumed isotropic since the fibres in the cementitious matrix orientate and distribute differently while concrete flows through the formwork. Therefore, the understanding of the fibres orientation and volumetric distribution in structural elements can help assessing the influence of fibres on properties such as the tensile strength of structural elements made of UHPSFRSCC.

The effect of fibre orientation on the mechanical response of Steel Fibre-Reinforced Self-Compacting Concrete (SFRSCC) and Steel Fibre-reinforced Concrete (FRC) has been studied in [1]-[3], to mention a few. Whereas the effect of fibre orientation on the tensile strength of UHPSFRSCC was evaluated by three-point bending tests in [4], which indicates the existence of a linear correlation between the fibre orientation and flexural tensile strength.

The experimental investigation presented in this article extends the knowledge of fibre orientation and its influence on the mechanical properties to the field of UHPSFRSCC. The main objective is to correlate the material's uniaxial tensile strength and fibre orientation, composing a set of diagrams fit for design purposes. For that, an experimental study based on a custom-designed direct tensile strength tests and image analysis was carried out.

2. EXPERIMENTAL PROGRAM

A batch of 150 litres of UHPFRSCC was prepared using the full-scale mixing station at Danish Technological Institute and a concrete slab with dimensions of 1350×1350×75 mm^3 was cast from a single pouring point as shown in Figure 1. The mixture has slump-flow of 550 mm, steel fibre content of 1.5% vol. (117 kg/m^3 - corrugated brass-coated steel fibres with length and diameter equal to 13.0 mm and 0.30 mm), and compressive strength of 190 MPa - measured on Ø100x200 cylinders after 28 days of curing immersed in water.

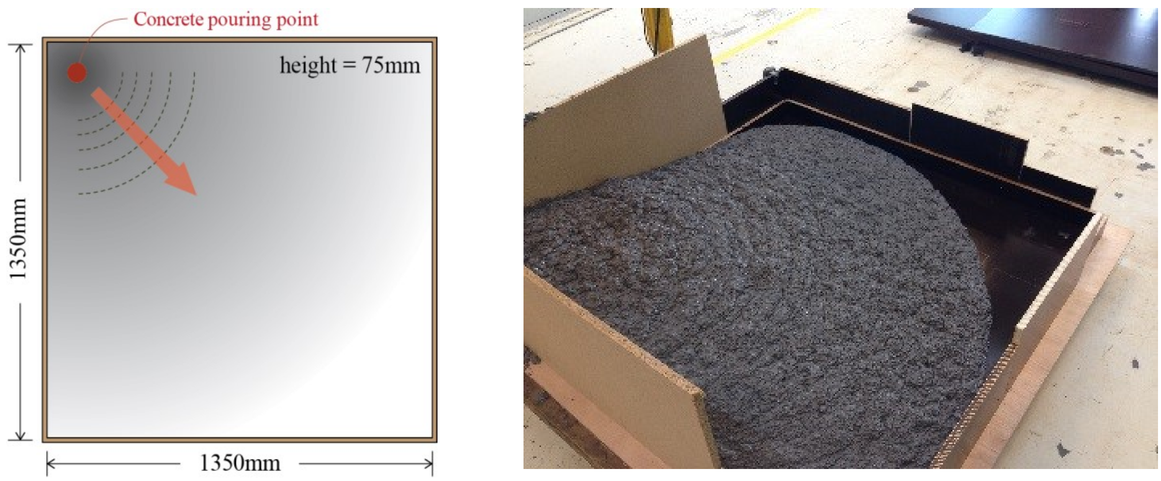

(a) (b)

Figure 1: UHPSFRSCC Concrete slab: (a) formwork and (b) image captured while concrete was flowing through the formwork.

Previous experience with casting steel fibre-reinforced concrete elements, supported by numerical simulations of the flow behaviour of SFRSCC, indicates that the fibre orientation in a slab cast using the casting procedure displayed in Figure 1 will vary considerably [5]. For example, Figure 2 illustrates the fibre orientation ellipsoids obtained from fluid dynamics-based simulations of SFRSCC flowing in a similar formwork [6]. These results (i.e. orientation ellipsoids) can be taken as a qualitative measure of the fibre orientation in this research and will be used as basis for the selection of the concrete samples to be tested.

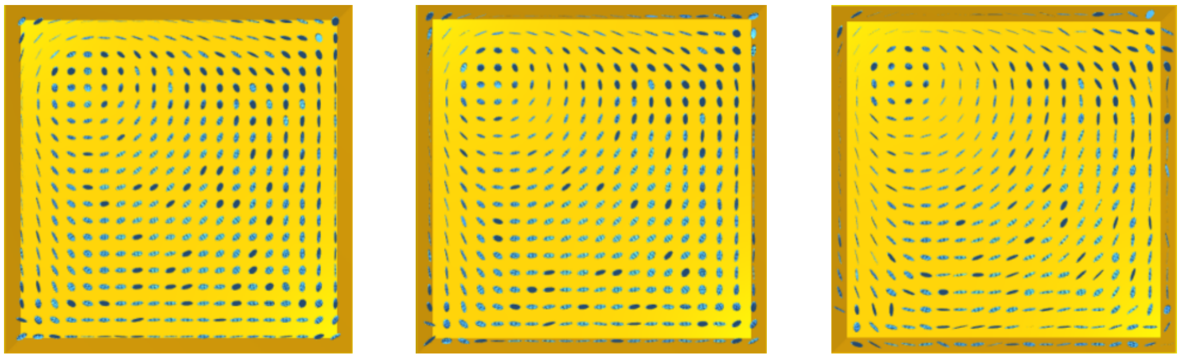

(a) (b) (c)

Figure 2: Fibre orientation ellipsoids at various horizontal planes of the concrete slab: (a) close to the bottom surface, (b) in the mid-plane and (c) close to the top surface.

Following 28 days of curing, the concrete slab was cut using a diamond saw into thirty prismatic samples (beams) with dimensions of 450×75×75 mm^3, representing a wide range of fibre orientation. The samples nomenclature and the results from the three-point bending tests – performed in accordance with EN 14651 [8] and published in [4] – are shown in Figure 3.

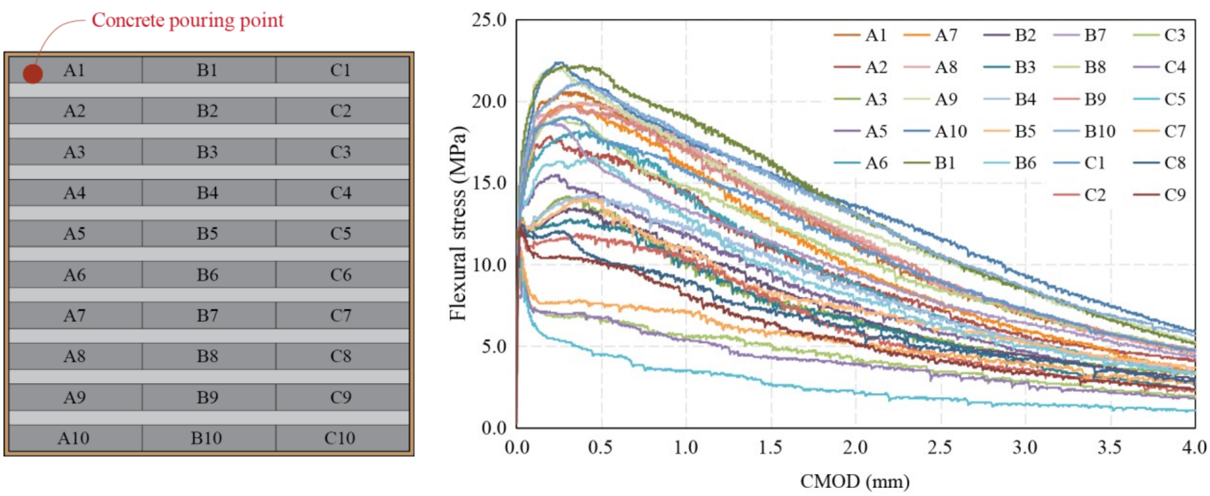

(a) (b)

Figure 3: (a) samples nomenclature and (b) corresponding three-point bending test results [4].

Based on the results from Figure 3 and the fibre orientation ellipsoids at the mid-plane of the concrete slab (Figure 2b), 10 samples covering a range of low to high tensile strength were selected. Specifically, the selected beams were A3, A5, A9, B1, B4, B10 and C3, C4, C5. Next, cubic samples (75×75×75 mm^3) were cut from the selected beams. At the age of 2 years, the samples were tested in a custom-designed direct-tensile strength test method. Notice that, this experimental program is a follow up of previous research [4], reason why the selected samples could not be tested at typical curing periods found in the literature.

The samples were notched on both sides (notch depth: 25mm) prior to performing the direct-tensile strength test. The introduction of a notch is required to a) generate a weak zone (tested cross-section: 75×25mm) where the crack opening occurs and b) allow for measuring the crack-mouth opening displacement, CMOD, and the notch gap as indicated in Figure 4.

After notching, the top and bottom surfaces of the samples were glued onto 95×95×25 mm^3 steel plates using epoxy resin. Both the concrete and the steel plate surface were cleaned thoroughly before the epoxy resin was applied to provide a proper bonding between surfaces. A steel rod was fixed to the plate and then mounted onto the testing machine where the tensile load was applied. The described scenario is depicted in Figure 4. Notice that the plate-rod connection is hinged in order to accommodate any rotation that might occur during testing, thus leading to a constant distribution of tensile stresses in the cross-section of the tested sample.

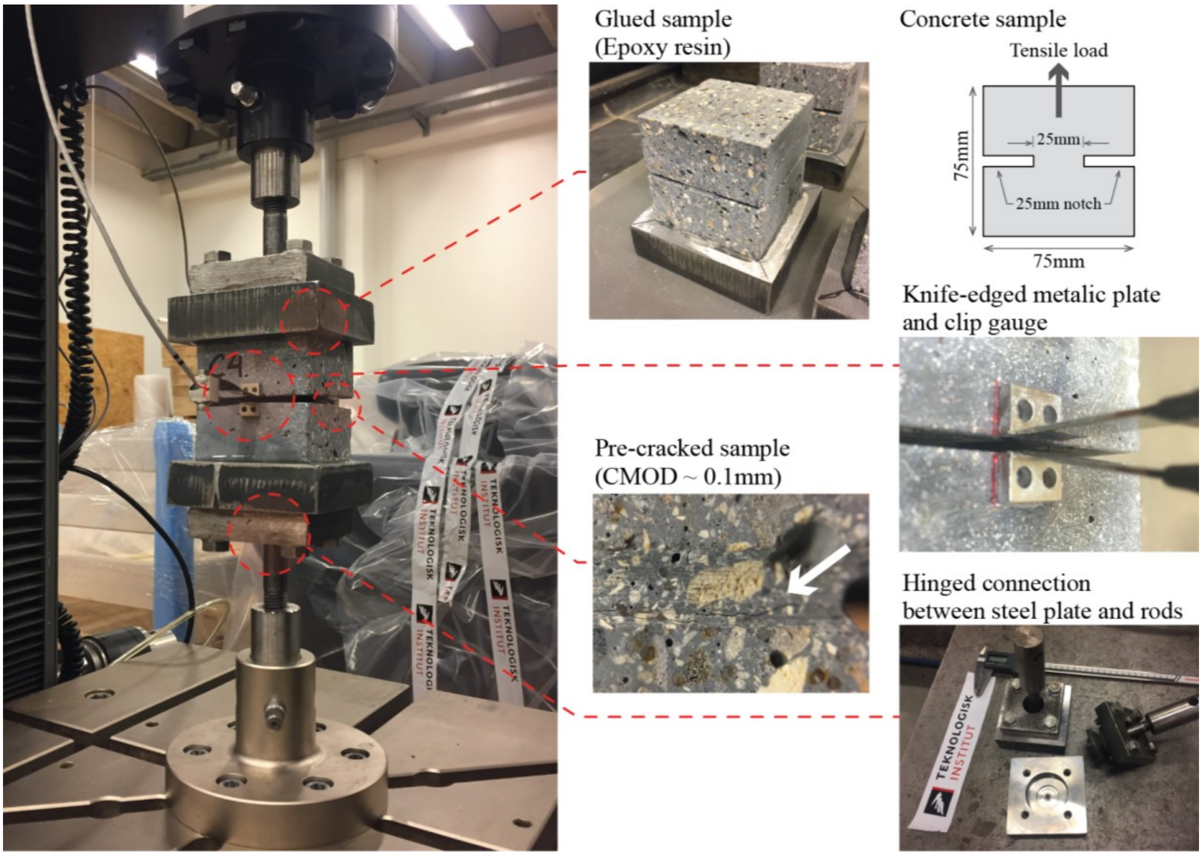

Figure 4: Experimental setup of the direct-tensile strength test.

Prior to applying load, the samples were pre-cracked (CMOD ~ 0.1mm) – an example is depicted in Figure 4. An Instron 5982 testing machine was used to perform the tests. The displacement rate (CMOD) was set at 0.2 mm/min – which is equivalent to the displacement rate specified in EN14651 [8] for CMOD > 0.1 mm. A built-in load cell recorded the load history, while two clip gauges (TLM Model UB-5A) placed at the notches recorded the CMOD. Knife-edged metallic plates (CONTROLS – Model 82-P0331/E1) that were glued around the notch held the clip gauge during testing. Details of the attached clip gauges are shown in Figure 4. A data logger attached to the testing machine recorded load and displacement during testing. The complete experimental setup for the custom-designed direct-tensile strength test method is depicted in Figure 4.

After testing, the samples were cut to expose the fibres in the tested cross-section, allowing for counting the number of fibres in the fracture plane. A high-resolution camera ImageSource – DKF23U274 captured digital images of both surfaces of a cross-section, which were evaluated by an image analysis method developed and validated in [4]. Basically, the method combines contrast enhancement, thresholding, and segmentation methods to count the number of fibres. Figure 5 illustrates the steps from the image analysis method for the sample B1. For each cross-section, two images were collected and the number of fibres, N_f, used in the subsequent analysis of fibre orientation was the average from the two images.

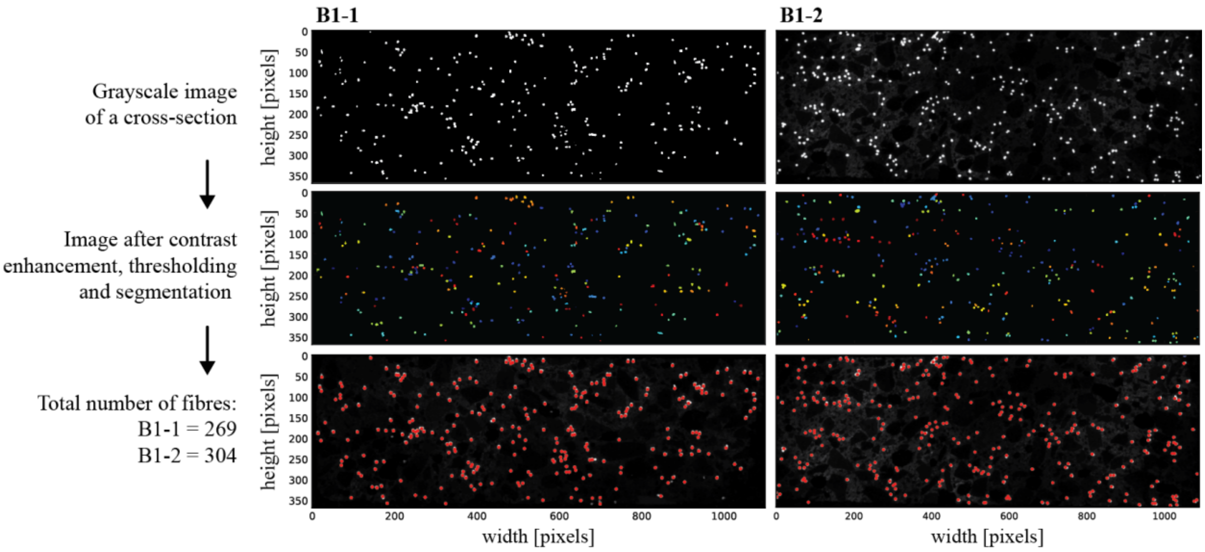

Figure 5: Image analysis identifying fibres in the cross-section of the sample B1-1.

Based on number of fibres, N_f, in a cross-section, the fibre orientation factor (α) reads [7]

$$\alpha = (N_f.A_f) / (V_f.A_C) , \tag{1}$$

where V_f, A_C, and A_f denote the fibre volume fraction, concrete area, and single fibre area.

The orientation factor represents the area of fibres relative to the maximum theoretical area of fibres crossing a given plane, i.e.:

- if $\alpha = 0$, no fibres cross a given plane (or all fibres are parallel to the plane)
- if $\alpha = 1$, all fibres are perpendicular to a given fracture plane.

3. RESULTS AND DISCUSSION

In the direct-tensile strength test, the tensile stress (σ_{CMOD}) at the cross-section reads

$$\sigma_{CMOD} = F_{CMOD} / A_C \, , \tag{2}$$

where F_{CMOD} is the load and A_C the cross-section in the notched zone of the concrete sample.

The direct tensile-strength test results, number of fibres (N_f) and fibre orientation factor (α) of the tested samples are shown in Figure 6.

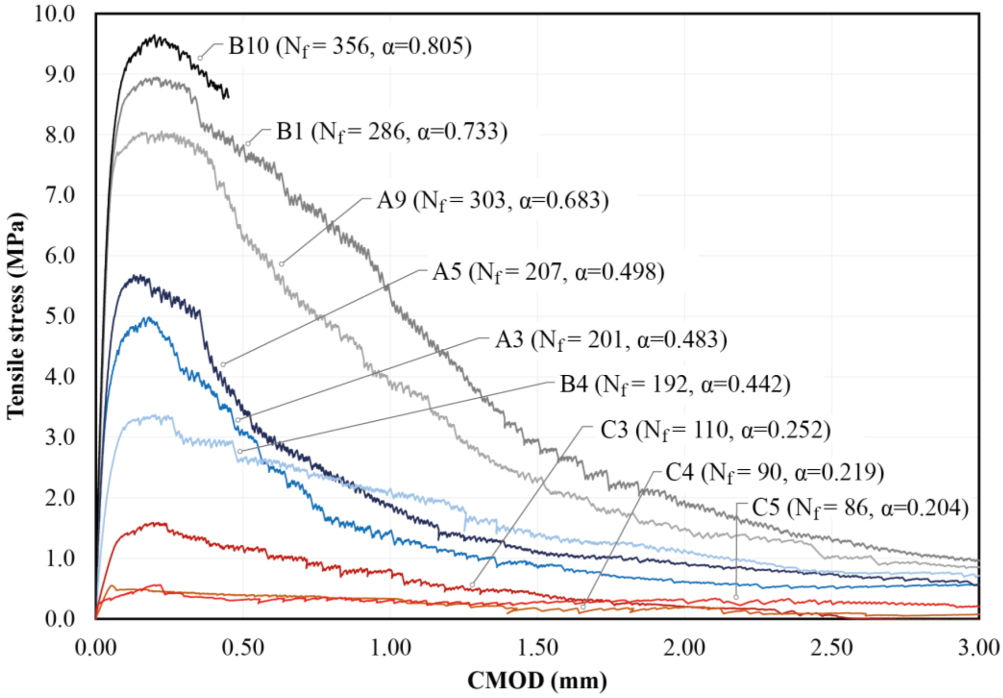

Figure 6. Direct-tensile strength tests: load-displacement curves as well as the corresponding average number of fibres and fibre orientation factor in the cross-section.

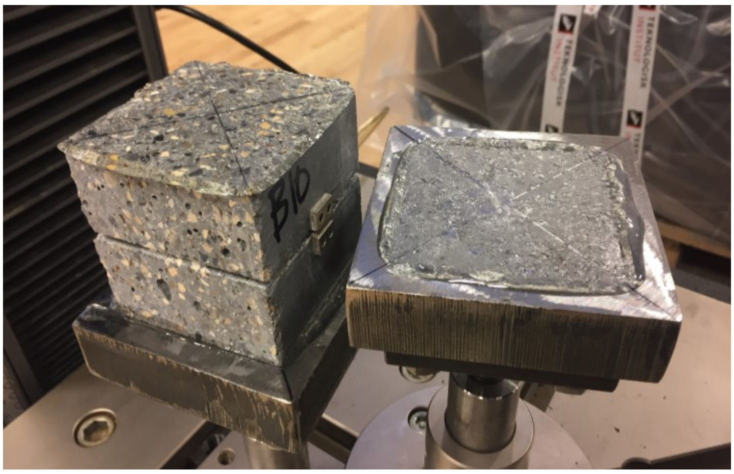

Figure 7: Detail of the failure in the interface between the sample and steel plate.

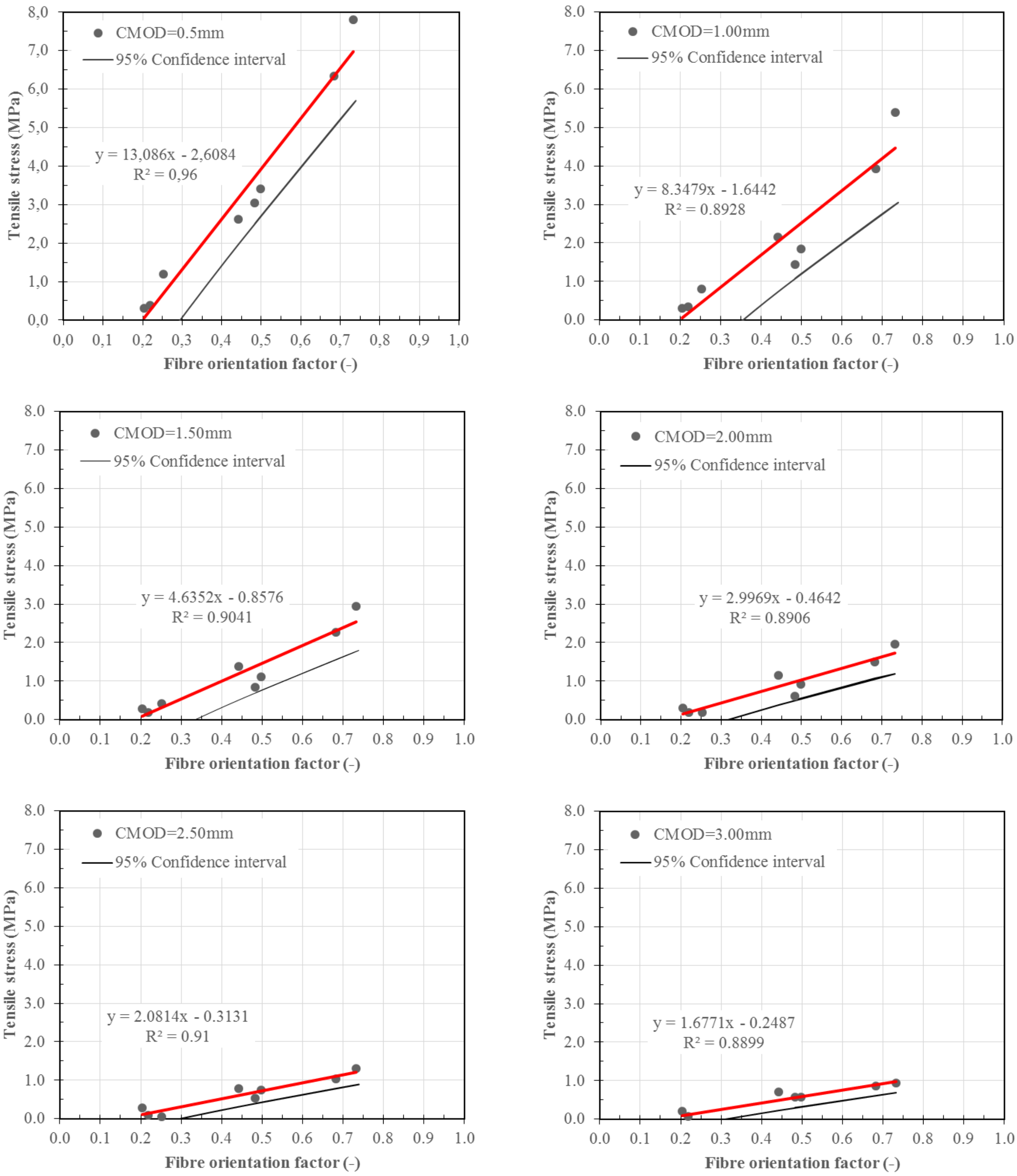

Figure 8: Design charts for CMOD ranging from 0.5 to 3.0 mm.

Notice that the results from B10 were partially recorded only due to the debonding of the sample during the execution of the test. Therefore, they were excluded from the analysis. The scenario after debonding is depicted in Fig. 7 and can be associated with a) the presence of impurities on the contact surface before the epoxy resin was applied or b) the limit bonding strength of the epoxy resin. The results from the direct-tensile strength tests (Fig. 6) indicate a clear influence of the fibre orientation factor on the mechanical response of the beams; i.e. locations where fibres are likely perpendicular to the cross-section exhibit greater tensile strength, while locations where fibres are likely parallel to the cross-section exhibit relatively lower tensile strength. The fibre counting (see N_f in Fig. 6) supports the obtained experimental results as well as the estimations from numerical simulations displayed in Fig. 2b. Specifically, the samples with high tensile strength (A9, B1 and B10) possess a greater number of fibres in the cross-section when compared to those with lower tensile strength (C3, C4 and C5). The design charts exhibiting the relation "α vs. σ_{CMOD}" for CMOD ranging from 0.5 to 3.0 mm are shown in Figure 8 and described by

$$\sigma_{CMOD} = a_1.\alpha + b_1 \tag{3}$$

The detailed results of the linear fit of experimental data are shown in Table 1. The minimum curve in Figure 8 was computed based on the standard deviation of experimental results and a 95% confidence level. The actual fibre volume fraction in one of the samples was found to be 1.42% [4]. Nonetheless, V_f was set at 1.50%, which is the nominal fibre volume fraction in the concrete composition. A detailed analysis of the linear and angular coefficients (i.e. a_1 and b_1 in Table 1) obtained for the design charts have a linear correlation with their corresponding CMOD. Hence, the individual design charts depicted in Fig. 8 can be grouped into a surface plot, as shown in Fig. 9. Such surface is expressed by Eq.(6), which was obtained as follows:

Step 1: The design chart coefficients from Figure 8 are computed by

$$a_1 = a_{1,1}.CMOD + b_{1,1} \tag{4}$$

$$b_1 = a_{1,2}.CMOD + b_{1,2} \tag{5}$$

Step 2: Eq.(4-5) as well as the values from Table 1 are applied to Eq.(1), thus

$$\sigma_{CMOD} = (-4.43\alpha + 0.93).CMOD + 13.22\alpha – 2.64 \tag{6}$$

Table I. Linear and angular coefficients from the design charts.

Figure 8				Figure 9					
[1]	[2]	[3]	[4]	Linear fit: [1] and [2]			Linear fit: [1] and [3]		
CMOD [mm]	a_1 [MPa]	b_1 [MPa]	R^2 [-]	$a_{1,1}$ [MPa/mm]	$b_{1,1}$ [MPa]	R^2 [-]	$a_{1,2}$ [MPa/mm]	$b_{1,2}$ [MPa]	R^2 [-]
0.5	13.09	-2.61	0.960	-4.43	13.22	0.866	0.93	-2.64	0.862
1.0	8.35	-1.64	0.893						
1.5	4.64	-0.86	0.904						
2.0	3.00	-0.46	0.891						
2.5	2.08	-0.31	0.910						
3.0	1.68	-0.25	0.890						

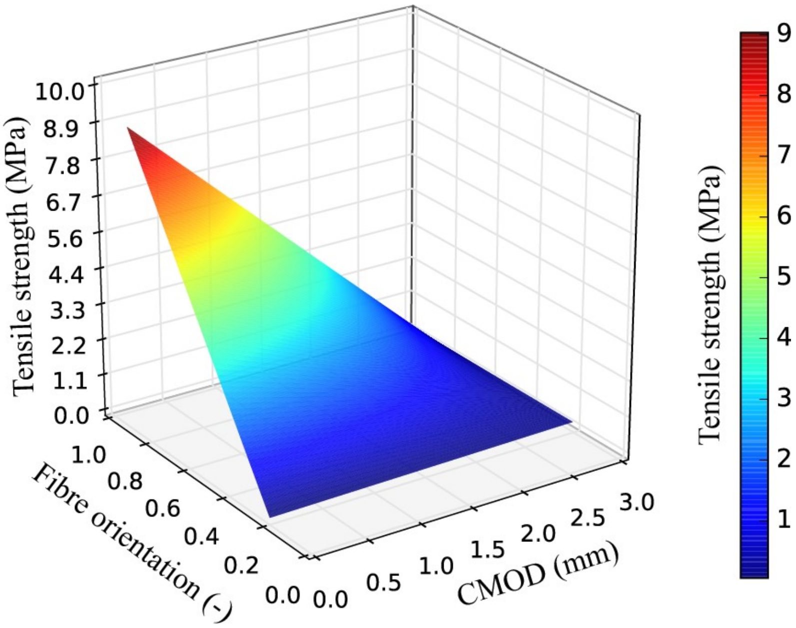

Figure 9: Design chart for $V_f = 1.50\%$.

4. CONCLUSIONS

The relation between fibre orientation and direct tensile strength of UHPSFRSCC was determined based on experimental results from a custom direct-tensile strength test method. Such relation was found to be similar to that of SFRSCC (linear relation) as well as the flexural strength of UHPSFRSCC published in [4]. The experimental results are presented in the form of design charts that can be used as a reference to estimate the tensile strength of concrete for a given fibre orientation factor and CMOD.

At present, the authors are considering a complementary study to the one presented in this paper. Such study includes investigations on the variability of the fibre volume fraction in concrete mass as well as testing (direct-tensile strength tests) the remaining samples from the UHPSFRSCC. The results from such study will be compared to those from [4] to establish the relation between the flexural and direct tensile strength in UHPSFRSCC.

REFERENCES

[1] Svec, O., Skocek, J., Stang, H., Olesen, J.F., Thrane, L.N., 'Application of the fluid dynamics model to the field of fibre reinforced self-compacting concrete', In Proceedings of the International Conference on Numerical Modelling Strategies for Sustainable Concrete Structures (SSCS), Aix-en-Provence, France, 2012.

[2] Gava, G.P., Pieri, T.S., Prudêncio Jr., L.R., 'Beam test of Steel fiber reinforced concrete: Influence of presence and position of notches and number of fibers in the cracked section', e-Mat - Revista de Ciência e Tecnologia de Materiais de Construção Civil. 1(2):114-127, 2004.

[3] Stähli, P., Custer, R. and Mier, J.G.M., 'On flow properties, fibre distribution, fibre orientation and flexural behaviour of FRC', Materials and Structures, 41(1):189–196, 2007.

[4] Leal da Silva, W.R., Svec, O., Thrane, L.N., Pade, C., 'Predicting fibre orientation and its effect on the mechanical properties of ultra-high performance steel fibre-reinforced self-compacting concrete', In Proceedings of ICSC | SCC 2016, Washington DC, USA, 2016.

[5] Danish Technological Institute, '4C-Flow', Denmark, 2015 (http://www.dti.dk/4c-flow/33808).
[6] Svec, O. and Skocek, J., 'Simple Navier's slip boundary condition for the non-Newtonian Lattice Boltzmann fluid dynamics solver'. J. of Non-Newtonian Fluid Mechanics 199(2013):61-69, 2013.
[7] Martinie, L. and Roussel, N., 'Simple tools for fiber orientation prediction in industrial practice', Cement and Concrete Research, 41(10): 993-1000, 2011.
[8] European Standard, EN14651, 'Test method for metallic fibre concrete. Measuring the flexural tensile strength (limit of proportionality (LOP), residual) ', 2005